Vibration of an Inflatable Fabric Wing Model

DONALD D. SEATH* AND ERNEST W. ANDERSON†

Iowa State University, Ames, Iowa

The vibrational characteristics of an inflatable, fabric wing model were found both experimentally and through the use of measured influence coefficients. The model tested had a semispan delta wing planform with 67.6° sweepback of the leading edge and a nearly uniform thickness. The first eight modes of vibration were experimentally determined for a range of internal wing pressures. The exciting force consisted of a loudspeaker located near the lower surface of the wing, driven by the amplified output of a variable-frequency, function generator. Flexibility influence coefficients were measured with the wing model subdivided into 10 and 18 sections and the natural frequencies and associated mode shapes for the first four modes of vibration determined by a matrix iteration procedure. The results obtained through experimental excitation and through the influence coefficient method were in reasonably good agreement.

I. Introduction

AT the present time there is a considerable amount of interest in inflatable space structures and winged re-entry vehicles that can be packaged in small containers for the launching operation and expanded when outside the earth's atmosphere. There have been several interesting investigations concerning plate-like fabric structures and their uses for space and re-entry vehicles. Leonard et al.[1] studied collapse loads and developed an analytical theory for the stress and deflection in inflatable fabric structures with particular application to platelike structures, such as could be used for re-entry vehicles. McComb[2] developed a linear theory for inflatable plates of arbitrary shape, and Stroud[3] compared the results obtained through application of this theory with the experimentally determined deflections and natural frequencies of vibration for a square Airmat plate with pinned and fixed boundaries.

The highly swept, delta planform design of the wing model used for this investigation was chosen because of its similarity to the planform for a re-entry vehicle. Knowledge of the static and dynamic characteristics of the primary structure of a vehicle is a necessary prelude to detailed design studies of landing loads, gust response, and similar aeroelastic phenomena.

The natural frequencies and mode shapes of a system can be found either experimentally or through the exact or approximate solution of equations, which mathematically represent the system. McComb[2] developed a linear, small-deflection theory for the elastic behavior of inflatable plates. His theory, however, does not include the added stiffness effects due to the curved edges of the wing or wing model, which, particularly at low internal pressures, have a noticeable effect upon the behavior of the structure.

Influence coefficients, either computed or measured, have been used successfully for finding approximate static deflections and vibrational characteristics of many types of elastic structures. This paper is concerned with an experimental investigation of the vibrational characteristics of an inflatable wing model. The resonant frequencies and mode shapes are determined both experimentally and through the use of measured influence coefficients.

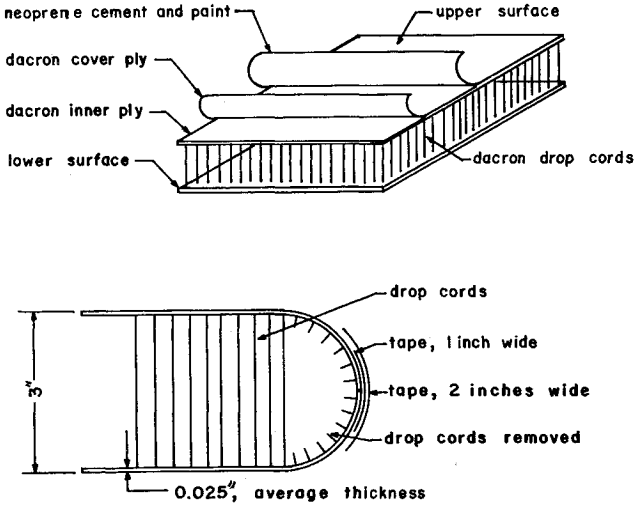

Fig. 1 Airmat and wing edge construction.

II. Inflatable Wing Model and Support

The Airmat fabric used in the construction of the inflatable wing model consists of two fabric surfaces tied together with drop cords. The cords hold the surface in a nearly parallel position when the wing is inflated. There are approximately 10 drop cords/in. in the spanwise direction and 6 drop cords/in. in the chordwise direction. Each surface consists of an inner ply of Dacron airmat weave and a cover ply of plain Dacron weave coated with neoprene cement to contain the inflating gas (Fig. 1).

The edges of the wing model were formed by cutting off the drop cords and bending the two surfaces into the form of a half cylinder. Fabric tapes were then used to splice the two ends together. The edge construction and the detailed dimensions of the airmat and tapes are shown in Fig. 1. Table 1 gives the weights of the materials used.

As is shown in Fig. 2, the wing model was constructed in the form of a semispan delta wing with 67.6° sweepback of the

Table 1 Material weights

Material	Weight
Airmat (including drop cords)	0.002335 psi
Airmat (without drop cords)	0.002024 psi
Tape, ½ in. wide	0.000331 lb/in.
Tape, 1 in. wide	0.000662 lb/in.
Tape, 2 in. wide	0.001325 lb/in.

Received January 6, 1966; revision received June 6, 1966.

* Instructor, Aerospace Engineering Department; now Assistant Professor, Aerospace and Mechanical Engineering Department, Arlington State College, Arlington, Texas. Associate Member AIAA.

† Professor and Head, Aerospace Engineering Department. Member AIAA.

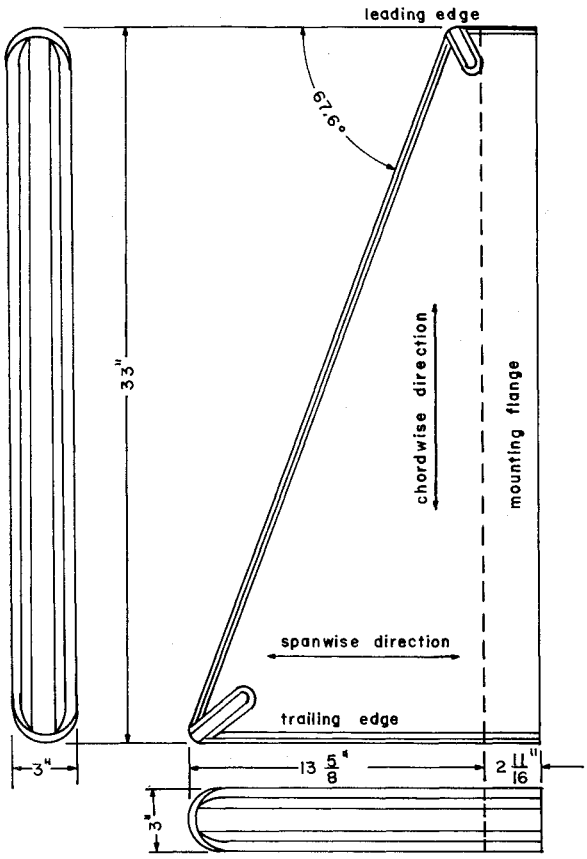

Fig. 2 Inflatable wing model.

leading edge and a nearly uniform thickness of 3 in. The root chord and semispan are 33 in. and 13 $\frac{5}{8}$ in., respectively. There is a 2 $\frac{11}{16}$ in. extension at the wing root for mounting purposes. This mounting flange is merely an extension of the upper and lower surfaces with the drop cords removed. The corners of the wing model were rounded and spliced, first with $\frac{1}{2}$-in. tape and then with 1-in. tape, and the entire wing was painted with aluminum paint.

The wing model was attached to a specially constructed steel support, which was in turn attached to two large vertical I-beams embedded in a concrete footing. The flange of the wing model was glued to the special steel support, and a $\frac{1}{2}$-in.-wide aluminum strip was used to bolt the flange to the support. Figure 3 shows a cross section of the wing and support, and Fig. 4 shows the wing attached to the support. Steel angle irons were used to clamp the wing root at the start of the drop cords and were held in contact with the model by the internal wing pressure, thus giving a clamped boundary effect. In addition to holding the model, the support, sealed the root of the wing so that the pressurizing gas could be contained, and two air inlet ports were provided. The inflatable wing model was designed, constructed, and donated by the Goodyear Aerospace Corporation of Akron, Ohio.

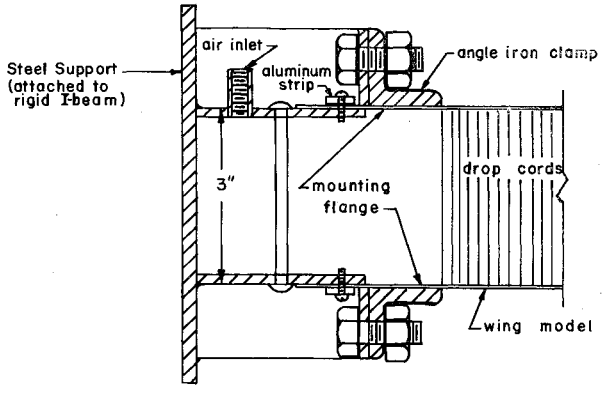

Fig. 3 Cross section of wing support.

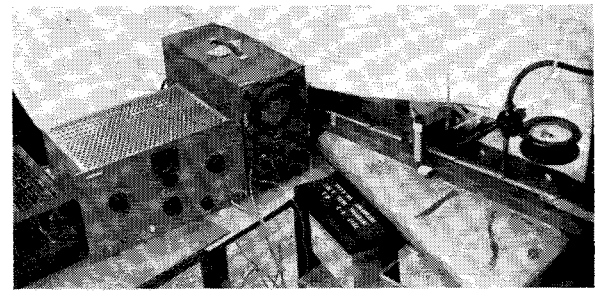

Fig. 4 Vibration test setup.

III. Vibration Tests

The purpose of the vibration tests was to experimentally find the natural frequencies of vibration of the wing model. Figure 4 shows the vibration test setup. In order to find the natural frequencies it was decided that a sinusoidal driving force should be applied to the wing, and the resonant frequencies would be determined by the response. It was found that the resonant frequencies were not affected by changing the position of the driving force and that only a small driving force was necessary when driving at a resonant frequency. These two facts suggested that the resonant frequencies were nearly the same as the natural frequencies.

Figure 5 shows the experimental equipment used for pressurizing the model. Because of the leakage between the model and the support, it was necessary to have a constant supply of pressure-controlled air entering the wing. Two regulators in series made it possible to regulate the wing pressure to within 0.02 in. of mercury. A mercury U-tube manometer was used to measure the pressure within the wing, a dial pressure gauge was used for approximate indications of pressure, and a thermometer was used to measure the air temperature in the wing. It was found that the air temperature inside the wing was the same as the temperature of the surrounding air. A dry air supply was used to prevent contamination of the inside of the wing.

Atmospheric pressure was obtained from a mercury barometer located in the same building as the test setup. The variations in barometric pressure and temperature did not have a noticeable effect upon the test results, and therefore average values of barometric pressure and temperature during the tests are shown with the results.

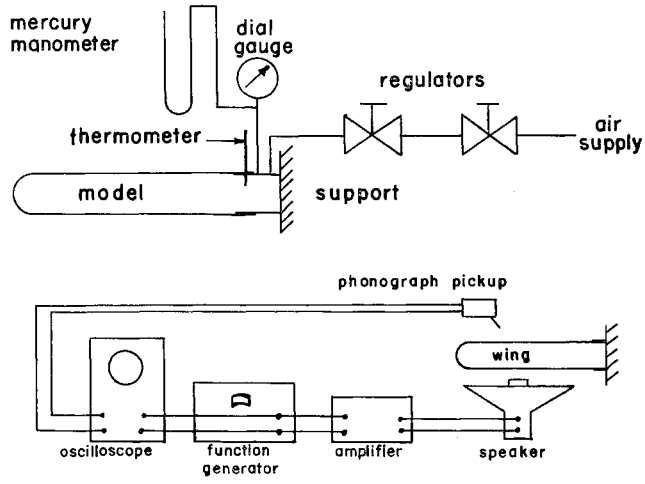

Fig. 5 Schematic of pressurizing system (top) and wiring diagram (bottom).

Experimental Resonant Frequencies, cps							
Mode	Wing Internal Pressure, psig						
	3	4	5	6	7	8	9
1	49.1	53.7	55.9	58.4	61.3	63.2	65.1
2	75.7	86.1	95.2	103.2	108.6	113.5	118
3	88.6	98.0	105.8	112	116	120	127
4	98.3	113	123	133	143	150	157
5	105.9	124	136	148	160	169	176
6	115.5	138	153	170	184	195	206
7	128	149	164	181	195	206	218
8	148	168	183	199	213	226	238

Average Barometric Pressure = 29.00 in. Hg
Average Temperature = 73°F

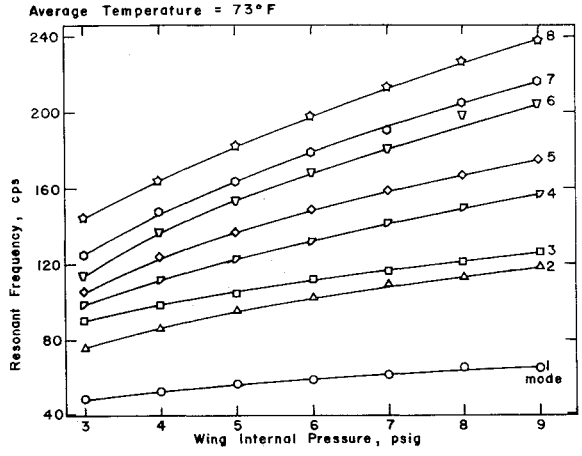

Fig. 6 Experimental resonant frequencies.

A 12-in.-diam, 25-w loudspeaker was used to excite the wing. The variable frequency sinusoidal signal obtained from a Hewlett-Packard model 202A function generator and amplified by a Knight 75-w model Kn-3076 booster amplifier was used to drive the speaker. Figure 5 shows the wiring diagram. It was found that this combination furnished more than sufficient power to excite the wing in all tests performed. The speaker, however, was modified by covering the face with a circular sheet of plywood with a 2 $\frac{1}{2}$-in.-diam hole in the center and a 1-in.-long section of a 2 $\frac{1}{2}$-in.-diam pipe inserted in the hole. This restricted the driving force to a smaller area and made it easier to determine the effect of the driving force position on the resonant frequency. The top of the pipe was positioned approximately $\frac{1}{2}$ in. from the lower surface of the wing.

A Dumont type 304-A oscilloscope was used in combination with a phonograph pickup to detect the frequencies at which the wing would resonate. The phonograph pickup was placed so that the needle just touched the wing surface. Then the output signal from the needle was impressed on the vertical sweep of the oscilloscope and the signal from the function generator was impressed on the horizontal sweep of the oscilloscope. Thus, it was possible to beat the frequency at which the wing was vibrating against the forcing frequency. When driven at any frequency other than a resonant one, the wing vibrated with a very low response amplitude. However, at resonance, all parts of the wing seemed to vibrate strongly at the resonant frequency. This enhanced response was indicated by an increase in the vertical amplitude on the oscilloscope trace.

The closest possible estimate of the natural frequency was determined in each case by reducing the power input to the speaker to the lowest value at which vibration could be observed while carefully adjusting the function generator frequency to give maximum response as observed on the oscilloscope. It was possible to read the function generator dial to the nearest 0.1 cps for frequencies up to 120 cps and to the nearest 1.0 cps for frequencies above 120 cps.

The measured experimental resonant frequencies excited by the speaker shaker are shown in Fig. 6. These are accurate to within 1%, the limiting accuracy figure of the function generator.

Figures 7–10 show the nodal patterns for the lowest eight modes of vibration for internal wing pressures of 3, 5, 7 and 9 psig, respectively. Pictures were also made for pressures of 4, 6, and 8 psig, but are not presented here. In some cases, in order to form the nodal patterns, it was necessary to move the driving force to avoid driving directly on a nodal line. Whole poppy seeds were used to form the nodal patterns because their color contrasted to that of the wing.

Several statements can be made concerning the experimental resonant frequencies.

1) The horizontal position of the driving force had no noticeable effect on the resonant frequency unless the driver was positioned near the leading edge of the root chord of the model. Then the resonant frequency showed an increase of as much as 1%.

2) The distance between the pipe section of the speaker-shaker and the lower surface of the wing had no noticeable effect on the resonant frequency except when the distance became less than $\frac{1}{2}$ in. Then the resonant frequency was lowered. This could be because the flat plywood baffle on the speaker produces a bounding plane close to the wing surface and thereby greatly increases the induced mass effect of the ambient atmosphere.

3) When the wing was excited in the first mode, the resonant frequency dropped approximately 1% as the amplitude of the driving force was increased by a factor of 10. The reason for this could be the same as that given for item 2.

4) The position of the phonograph pickup, either on the wing model surface or on the root support, showed no measurable change in the resonant frequency.

IV. Influence Coefficient Method

One method of finding the natural frequencies of vibration with small deflections, as described in Bisplinghoff et al.,[4] is that using lumped masses and flexibility-influence coefficients. In this method the wing is divided into sections, and the mass of each section is assumed concentrated at its

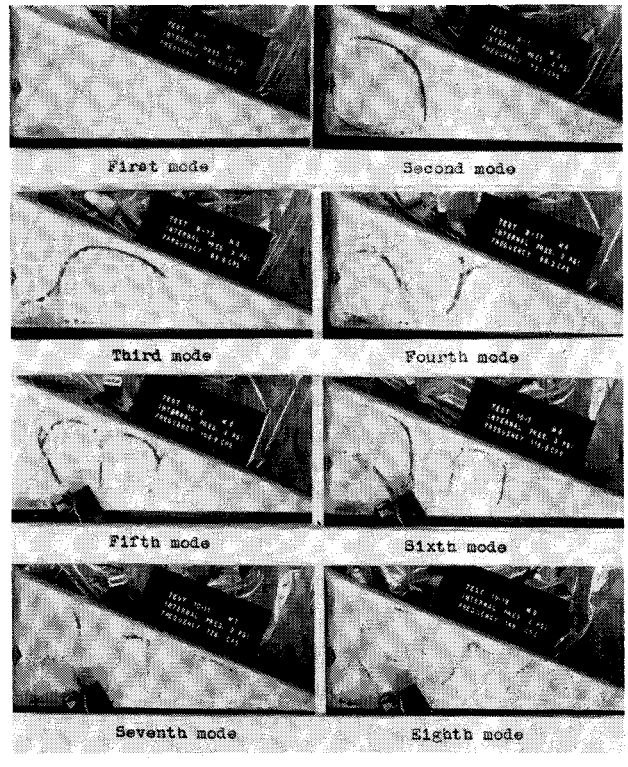

Fig. 7 Photograph of nodal patterns for 3 psig internal wing pressure.

center of gravity, so that the wing is replaced by a weightless system carrying the lumped masses at discrete stations.

The matrix equation representing the transverse deflections of the wing is

$$(W)/\omega^2 = (D)(W) \tag{1}$$

where

$$(D) = (C)(M) \tag{2}$$

ω is the natural circular frequency, the elements of the column matrix (W) are the ordinates of the mode shape, the elements of the square symmetric matrix (C) are the influence coefficients C_{ij} (the deflection at the ith station due to a unit load at the jth station), and the elements of the diagonal matrix (M) are the section masses.

In order to substantiate the theory that accuracy increases as the number of sections increases, the wing was first divided into 10 sections and then into 18 sections.

The section masses used in Eq. (2) included the mass of wing materials, the mass of air inside the wing, and the virtual mass of external air. Mass of the wing materials was computed from data presented in Table 1. The mass of the internal air was computed using the gage pressure plus 29.00 in. of mercury for an average value of barometric pressure and 73° for an average value of temperature inside the wing. The use of these average values did not introduce any appreciable errors for the operating ranges of barometric pressure and temperature observed during the tests. The virtual mass of external air was assumed equal to the mass of air displaced by the wing.

Influence coefficients were measured directly. In order to do this, a sequence of vertical loads was applied in turn at each of the sections, and for each loading the corresponding deflection at each section, including that at the loaded section, was measured. The procedure is outlined below.

First, an initial load was applied to remove any slack in the system, and then several successive loads of at least 100-g increments were applied and then withdrawn. For each load the displacements were measured with a Brown and Sharpe micrometer head attached to a beam which in turn was attached to the wing support. By means of a battery and light circuit, which was closed when the micrometer made contact with a small copper plate attached to the surface of the wing, deflections could be measured to the nearest 0.00005 in.

It was found that applying the load to the wing surface through a $\frac{3}{8}$-in. sphere did not result in equal deflections of the upper and lower surfaces. Hence, various sizes of $\frac{1}{8}$-in.-

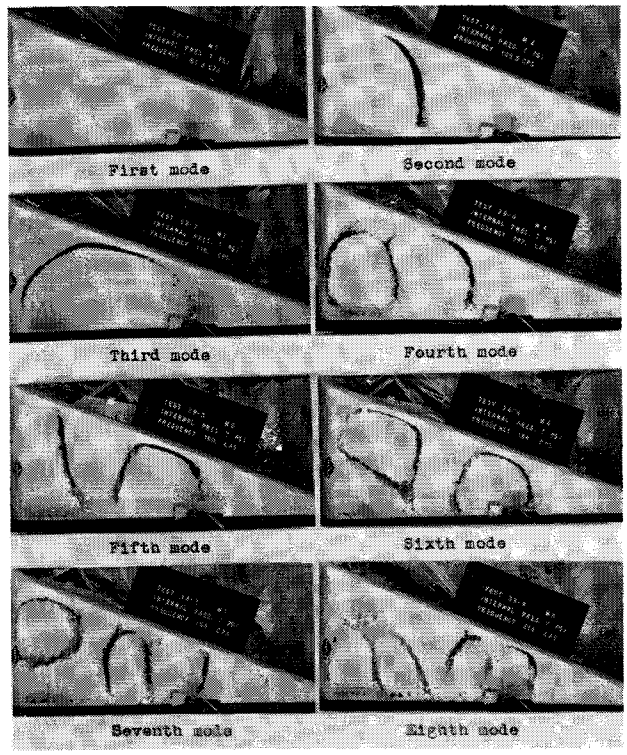

Fig. 9 Photograph of nodal patterns for 7 psig internal wing pressure.

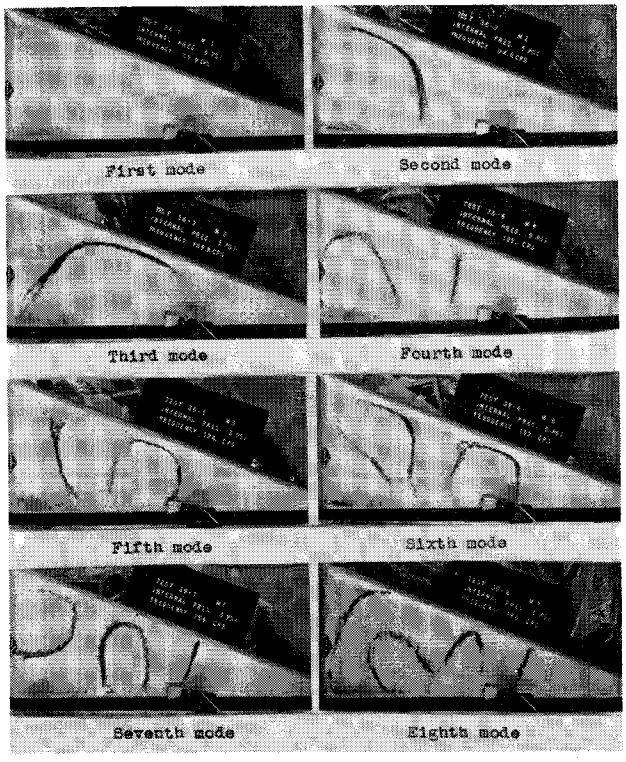

Fig. 8 Photograph of nodal patterns for 5 psig internal wing pressure.

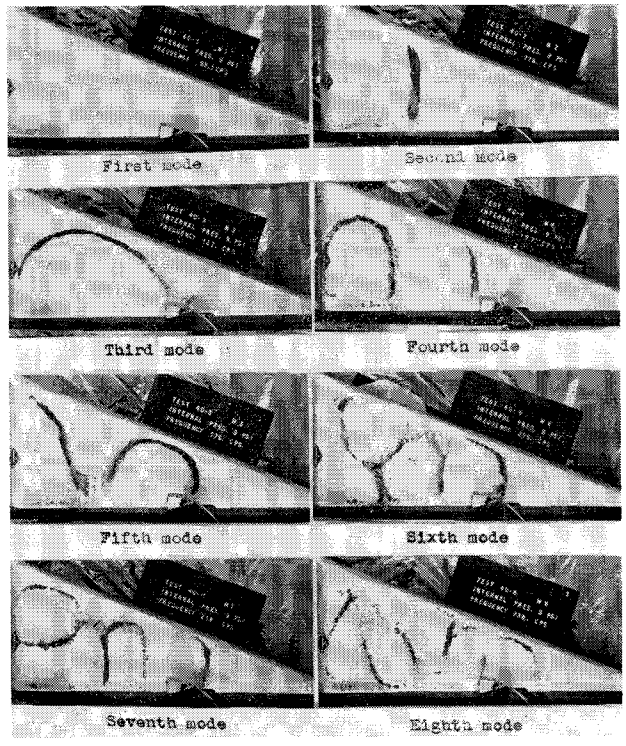

Fig. 10 Photograph of nodal patterns for 9 psig internal wing pressure.

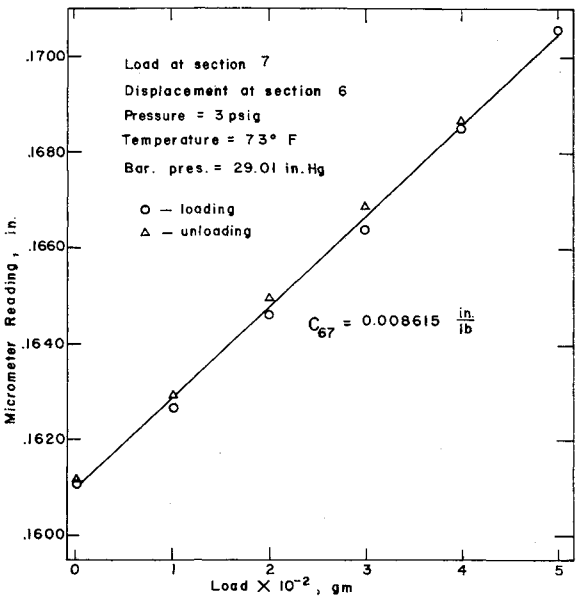

Fig. 11 Graph of load vs displacement used for determining influence coefficients.

thick plastic plates were tried between the loading point and the wing surface, causing a distribution rather than a point application of the load. A plastic plate, 1-in. square or larger, produced equal deflections of the upper and lower surfaces. Because of the large size of the wing sections when only 10 subdivisions were used, a plastic plate 2-in. square was employed for loading. This produced a deflection that seemed to represent more nearly the average deflection of the loaded section. Whether or not a plate was used had no noticeable effect on the deflections at sections other than the one at which the load was applied.

Total loads were kept as small as possible in an attempt to produce deflections of the same order of magnitude as those produced when the wing was excited and to avoid any wrinkling of the wing surfaces. However, it was necessary to apply loads of sufficient magnitude to produce deflections

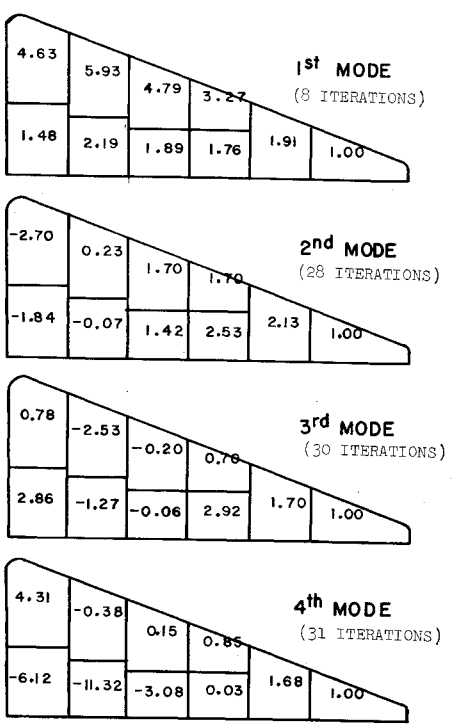

Fig. 12 Ordinates of the mode shapes for the first four modes at 7 psig internal wing pressure using 10 sections.

large enough to reduce the errors in reading the micrometer. To do this, it was necessary with each loading increment to produce an incremental deflection of at least 0.0010 in. This resulted in errors of 10% or less for each deflection measurement reading. The loading weights used were checked on a balance and found to be within 1% of their represented values. Figure 11 shows a load-deflection curve used for determining influence coefficients.

It can be shown[5] by the reciprocal deflection theorem that the matrix of influence coefficients is theoretically symmetrical, i.e., $C_{ij} = C_{ji}$. However, the experimentally measured values of C_{ij} sometimes differed from the corresponding values of C_{ji} by as much as 10%. Therefore, the values of C_{ij} and C_{ji} were averaged to form a symmetrical matrix of influence coefficients.

Table 2 shows the natural frequencies as computed by the influence coefficient, matrix-iteration method. These are indicated for both the 10-section subdivisions and the 18-section subdivisions and experimental values are also indicated.

Iterations and sweeping operations used in finding the natural frequencies were performed with the Iowa State University Cyclone Digital Computer, which operates with binary numbers and carries eight significant numbers. The iteration process for each mode was begun with all elements of the column matrix (W) set equal to unity, and continued until the frequency resulting from the ith iteration differed from the frequency resulting from the (i-1)st iteration by less than 0.03 cps. Figure 12 shows the resulting ordinates of the mode shapes and number of iterations for convergence for 7 psig internal wing pressure and 10 sections and Fig. 13 for 7 psig internal wing pressure and 18 sections.

Flomenhoft[6] pointed out the possibility of iteration errors in modes above the fundamental, arising from small differences of large numbers that are not carried by the calculating equipment. To overcome this, he advised arranging the sweeping operation so that the section with the largest product of mass times mode-ordinate would be swept out.

His advice was followed because in the initial arrangement, wherein an arbitrary section (not the one with the largest product) was swept out, the computation of the second mode for the wing divided into 18 sections resulted in a nodal line that was nearly perpendicular to the experimentally observed position of the nodal line. After rearranging so that the sweeping operation would sweep out the section with the largest product, the position of the nodal line agreed quite well with that determined experimentally. The effect on the natural frequency was not so drastic, changing its value by only a few per cent.

V. Discussion

As illustrated in Fig. 6, the resonant frequency for each mode increases with an increase in the gage pressure of the air inside the wing. A graph of the experimental data on log-log graph paper shows that frequency is proportional to the gage pressure raised to the 0.216 power for the first mode, 0.427 for the second mode, 0.425 for the fourth mode, and 0.430 for the eighth mode. Stroud[3] found that, for the higher modes of a 1-in.-thick, square, inflatable plate clamped on

Table 2 Natural frequencies by influence coefficient method, cps

Mode	Internal wing pressure, psig			
1	46.1[a] (49.1)[b]	53.4[a] (55.9)[b]	58.0[a] (61.3)[b] [60.2][c]	62.2[a] (65.1)[b]
2	67.4[a] (75.7)[b]	85.8[a] (94.6)[b]	91.3[a] (108.6)[b] [96.7][c]	100.2[a] (122)[b]
3	71.0[a] (88.6)[b]	94.7[a] (105.8)[b]	104.8[a] (116)[b]	115.6[a] (127)[b]
4	71.0[a] (98.3)[b]	91.8[a] (123)[b]	105.4[a] (143)[b]	117.5[a] (157)[b]

[a] Using ten wing sections.
[b] Experimental value.
[c] Using eighteen wing sections.

all edges, the resonant frequency is proportional to the gage pressure raised to the 0.500 power.

An examination of the photographs of the nodal patterns revealed some interesting phenomena. Comparison of the patterns for the second mode as the wing internal pressure is increased shows a straightening of the nodal line in the spanwise direction and a disappearance of the line near the curved edge of the model until the vibration appears to be predominantly torsional in character. This is probably because, at lower pressures, the stiffness of the curved edge of the wing is a significant part of the total stiffness; however, as the pressure is increased, the edge stiffness becomes less and less important as compared to the shear stiffness due to the internal pressurized air. For the third mode the nodal line runs predominantly in spanwise direction at 3 psig, but as the pressure is increased the nodal line swings around until, at 9 psig, it runs predominantly in a chordwise direction, indicating characteristics similar to those of a second bending mode of vibration. This is probably also a result of the decreasing importance of the edge stiffness. Examination of other nodal patterns reveals similar changes. Thus, as the internal pressure is increased, the edge effects become less and less important and the inflated wing acts more and more like a uniform plate. Another reason for the change in nodal patterns with increasing pressure is that the pressure also influences the relative importance of extension of the upper and lower surfaces and transverse shear. A log-log plot of frequency squared vs pressure reveals that in the first mode the elastic constants of the fabric predominate and at higher modes the transverse shearing stiffness of the model predominates.[7]

Application of the influence coefficient method, using 10 sections, resulted in natural frequencies within 6% of the experimental frequencies for the first (or fundamental) mode. The use of 18 sections improved this to 2%, thereby illustrating the increase in accuracy obtained by an increase in the number of sections.

Difficulties were encountered in applying loads and measuring the deflections of a section when the center of gravity of the section fell on the curved portion of the edge of the model. This may have introduced errors, amount unknown, especially for the case of 18 sections where the centers of gravity of 10 of the sections fell on the curved edges. A more judicious arrangement of sections would cause fewer centers of gravity to fall on the edges.

The authors feel that the use of the influence coefficient method worked satisfactorily for finding the natural frequencies of vibration of the inflatable wing model. This is particularly true when one considers the possible increase in accuracy that would be obtained by the use of a larger number of sections, judiciously chosen.

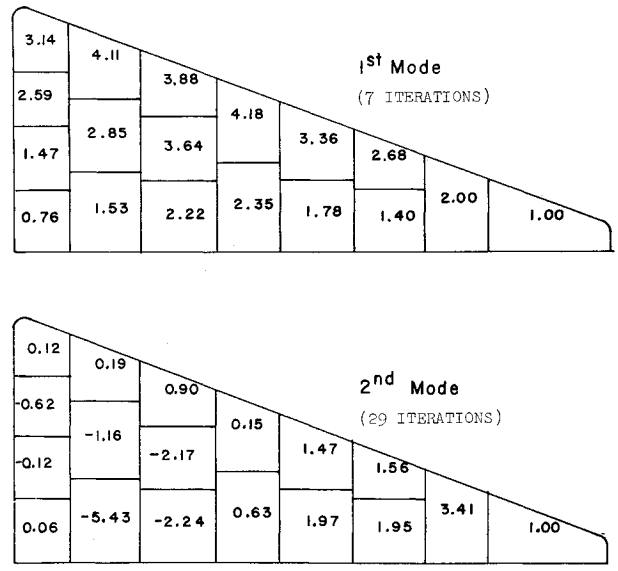

Fig. 13 Ordinates of the mode shapes for the first 2 modes at 7 psig internal wing pressure using 18 sections.

References

[1] Leonard, R. W., McComb, H. G., Jr., Zender, G. W., and Stroud, W. J., "Analysis of inflated reentry and space structures," *Recovery of Space Vehicles Symposium* (Institute of Aeronautical Sciences, New York, 1960), pp. 62–78.

[2] McComb, H. G., Jr., "A linear theory for inflatable plates of arbitrary shape," NASA TN D-930 (1961).

[3] Stroud, W. J., "Experimental and theoretical deflections and natural frequencies of an inflatable plate," NASA TN D-931 (1961).

[4] Bisplinghoff, R. L., Ashley, H., and Halfman, R. L., *Aeroelasticity* (Addison-Wesley Publishing Co. Inc., Reading, Mass., 1955), Chap. IV, pp. 164–169.

[5] Fung, Y. C., *An Introduction to the Theory of Aeroelasticity* (John Wiley & Sons Inc., New York, 1955), Chap. 1, p. 22.

[6] Flomenhoft, H. I., "A method for determining mode shapes and frequencies above the fundamental by matrix iteration," J. Appl. Mech. **17**, 249–256 (1950).

[7] Stevens, C. D., private correspondence to E. W. Anderson from G. L. Jeppesen, Goodyear Aircraft (1963).